Ocean Engineering 235 (2021) 109423

Contents lists available at ScienceDirect

Ocean Engineering

journal homepage: www.elsevier.com/locate/oceaneng

Uncertainty in the real-time estimation of ship speed through water

Øyvind Øksnes Dalheim *, Sverre Steen

Department of Marine Technology, Norwegian University of Science and Technology (NTNU), Otto Nielsens vei 10, 7491 Trondheim, Norway

ARTICLE INFO

Keywords:
Speed through water
Doppler speed log
Sea current
Uncertainty
Monte Carlo simulation

ABSTRACT

The ship speed through water (STW) is a critical variable for evaluation of ship performance. With a cubic relation to the expected shaft power, even small inaccuracies in measured STW amplifies to more considerable inaccuracies in the expected shaft power. STW is traditionally measured using a speed log, more specifically by the Doppler acoustic speed log principle. The stability and precision of this technique is however questionable, particularly when ships are exposed to waves. For ships equipped with sensors and instrumentation for measuring propulsion related data, the STW can be estimated from in-service measurements on the propeller shaft. An accuracy of this STW estimate similar to the speed log will increase the overall confidence in the ship performance evaluation. In this paper we study the uncertainty in the estimated STW using propeller loading measurements, and identify the most critical components of ship instrumentation in order to achieve an estimate of STW with sufficient accuracy. The uncertainty analysis includes a fixed pitch and controllable pitch propeller, influence from including a thrust sensor and influence from waves on the expected uncertainty in estimated STW. The uncertainty in estimated STW is found to be similar to the uncertainty provided by manufacturers of Doppler speed logs. The propeller pitch angle is found to have a significant contribution to the total uncertainty in STW. Including thrust measurements decreases the uncertainty in STW by 34%, and the uncertainty is found to be not very much affected by the presence of waves.

1. Introduction

Accurate measurements of ship speed through water (STW) are important in various applications e.g., ship performance monitoring, hull monitoring, optimization of ship design and operation, speed trials, sea state identification etc. Relative to fuel consumption or consumed shaft power, the STW forms a single explicit proof of how efficient the ship moves through the water. In waters with no current, the STW equals the speed over ground (SOG). In presence of a longitudinal current speed u_v however, the STW equals SOG - u_v. A traditional ship performance analysis evaluates the performance in terms of ship speed vs power, e.g. as a simple speed–power scatter plot, by regressing propulsion power on the ship speed or in terms of statistically analyzing the excessive use of power relative to a baseline power requirement, mainly calm water. In either case, the need for accurate STW measurements is stated through the cubic relationship between shaft power and the attainable speed. The cubic dependency implies that even small variations in STW will have significant impact on the required propulsion power. In terms of ship performance, this means that the resolution of detectable changes in performance is directly linked to the uncertainty in the STW.

With the increased focus on greenhouse gas emissions (IMO, 2009, 2011, 2012; ITTC, 2014a), STW measurements are becoming more relevant in terms of validating ship performance in real operational conditions, as well as for optimizing ship design and operation. Similar is seen in connection with sea state estimation, which has been giving more attention to the extent of which the measurement uncertainty affects the calculation of the motion transfer functions (Nielsen and Dietz, 2020). Considering how the ship speed relates to propulsion power to the power of three, the need for precise and reliable measurements of STW is indisputable. The same argument holds for the sake of validating the change in fuel efficiency after installing fuel saving devices such as a bulbous retrofit, wave foils, fuel saving propeller attachments, wing sails or Flettner rotors as well as after doing regular hull and propeller cleaning. In any case, measuring STW with very limited uncertainty is critical for the sake of facilitating deeper knowledge of ship performance, not to mention for obtaining a thorough knowledge base for optimization of ship design and operation.

Traditionally, speed through water is measured using a speed log. Over the years, a number of techniques are established as industrial practice, but the most common are the Electromagnetic (EMCP), the Acoustic Correlation (ACCP) and the Acoustic Doppler (ADCP) current profilers, often referred to as speed logs (van den Boom and Hasselaar, 2014), the latter by far the most common. The working principle of an

* Corresponding author.
E-mail address: oyvind.dalheim@ntnu.no (Ø.Ø. Dalheim).

https://doi.org/10.1016/j.oceaneng.2021.109423
Received 13 April 2021; Received in revised form 1 June 2021; Accepted 27 June 2021
Available online 2 July 2021

ADCP is to calculate speed relative to the water from the measured Doppler frequency shift in ultrasound pulses transmitted from the hull. The pulses are reflected by impurities in the water, or density differences ("layers") . Despite its frequent use, several recent studies are concerned with the accuracy of speed logs (Griffiths and Bradley, 1998; Bos, 2016; Antola et al., 2017; Hasselaar and den Hollander, 2017; Taudien and Bilen, 2018; Ikonomakis et al., 2019; Prytz et al., 2019). van den Boom et al. (2013) states that the speed log is one of the most inaccurate measurement devices onboard ships. The concerns relate to several aspects of the measurement technique. First of all, as the water flow close to the hull is altered by the presence of the ship, it is essential to only consider ultrasound pulses reflected at a certain distance away from the hull, at least outside the boundary layer. This will vary with draft and trim. The speed log might however switch to bottom tracking if the tracking depth is set far beneath the ship and the ship enters shallow waters. From a hydrodynamic point of view, it is also questionable whether the measured STW actually corresponds to the water passing speed that is relevant for the ship. This becomes even more relevant in sailing environments having a large vertical gradient of the prevailing current. In other words, despite the speed measured by the speed log being accurate at the current tracking depth, it is not necessarily the same speed as experienced by the hull. Additionally comes issues directly concerning the sensor accuracy. A speed log needs to be calibrated, but the calibration might depend on externalities such as temperature. If the speed log experiences sensor drifting, in-service recalibration will be required. There are however no obvious ways of recalibrating a speed log for a ship in-service. Other concerns directly related to the accuracy of a speed log are given in Taudien and Bilen (2018), addressing the total long-term accuracy of six different Doppler speed log configurations along with experimental validation in a tow tank. Taudien and Bilen (2018) reports a worst case sum of the separate error terms between 0.550% and 1.005% for a 300 kHz leveled Doppler instrument, while between 0.745% and 1.193% when including 20° pitching of the instrument. As mentioned, it is commonly experienced that speed logs are not providing sufficient measurement accuracy. As the Doppler measuring technique assumes that the scatterers in the water are moving in a constant, uniform motion, the quality of the measurement will degrade along with violating this assumption, e.g. in turbulent flow. Likewise, the measurement accuracy will be influenced by acoustic noise pollution in the surrounding environment from e.g., breaking waves, engine noise, and turbulent pressure fluctuations in the flow (Wanis et al., 2010). The measurement accuracy is also influenced by ship motions causing aeration (Ikonomakis et al., 2019). In the presence of air bubbles, false reflections of ultrasound pulses might enter the speed log, which will have a direct impact on the measured STW.

Along with a growing interest in ship energy efficiency evaluation and emission control, it is gradually becoming more common to equip ships with sensors and data acquisition systems in order to do in-service monitoring (Dalheim and Steen, 2020). With that comes new opportunities to extract valuable information from ships in operation, which in turn has helped raise concerns about the accuracy of speed logs. Recent literature has therefore started focusing on estimating STW using various in-service measurement data, with the aim of overcoming the erratic behavior of speed logs as well as to provide better accuracy than what is experienced from speed logs. Antola et al. (2017) developed a virtual speed log that combined propulsion related data, speed over ground (SOG), speed log data and current forecasts in order to improve the STW measurements. The virtual speed log was modeled as a state space model evolving as a random walk. The results showed that the model was able to reduce the scatter in STW relative to the forecast STW (calculated from SOG and the current forecast), and that the accuracy was superior compared to speed log data. As a general assumption, the inflow to the propeller was considered undisturbed, i.e. no wake, which is a fairly rough assumption (Pecoraro et al., 2015). Secondly, the added resistance in wind and waves, denoted R_A, was assumed small compared to the calm water resistance R_{CS}, which means that the observational equation including the added resistance could be solved as a perturbation series in R_A/R_{CS}. This is also to be considered a rough assumption, given the large variations in added resistance experienced by ships having e.g. a length of approximately 100 m (Dalheim and Steen, 2020). Further on, Ikonomakis et al. (2019) developed a somewhat similar virtual speed log. Rather than relying on knowledge of the ship's calm water resistance, this virtual speed log combined onboard inertial measurements and external hindcast sea current measurements into a kinematic model of vessel motions in order to estimate the STW. The model improved the estimated STW compared to measurements provided by the speed log. Brandsæter and Vanem (2018) validated various regression models to predict a ship's STW based on full scale sensor measurements, including environmental forces. STW prediction by data regression relies however on a training data set, and does not resemble a STW estimation model in the sense of its independency of dedicated STW measurement devices, such as speed logs.

In terms of practical applications as well as for research objectives, the STW is a fundamental variable concerning several types of analyses and optimization tasks connected to ship performance. Considering the sensitivity of STW relative to relevant dependent variables, the STW stands out as one of the most important measures onboard a ship. With reliable measurements of both STW and SOG, the one dimensional (1D) sea current along the longitudinal axis of the ship can be calculated from the difference in SOG and STW. Recent developments in sea current modeling have resulted in sea current forecast models having high temporal and spatial resolution, e.g. the Norwegian coastal model NorKyst-800 (Albretsen et al., 2011). Such forecast models might provide important input to e.g. equipment for route planning. In the InnoCurrent project, the aim is to address possible ways of reducing fuel consumption by making use of high fidelity sea current forecast models such as the NorKyst-800 model, with focus on selecting a preferred route in terms of sailing distance and sea current. If however the route is to be planned according to a forecast of the sea current, it is important to know the uncertainty of the predicted sea current. It is only by considering the uncertainty that the route planning tool can make informed decisions regarding the preferred sailing route. The sea current forecast models are however depending on data for validating the models. The idea of using the ship as a sensor is therefore tempting, as the ship can provide a continuous stream of validation data, at various locations. With access to a large fleet of ships in operation, recent advances in sensor fusion technologies makes it even possible to provide a more complete and rather detailed picture of how the sea current varies, both temporally and spatially. This is a similar application as can be found in research concerning e.g. environmental monitoring (Berman et al., 2020).

Even though estimating STW from in-service measurements might possibly improve the estimate of STW as compared to speed logs, there is a clear gap in knowledge regarding the uncertainties related to such estimates. If the intention is to use in-service measurements for validation purposes, e.g. for validation of sea current forecast models, it is essential to acquire knowledge about the uncertainty in the STW estimation, and thereby the longitudinal sea current based on ship in-service measurements. In this paper, we address the uncertainty in estimating STW from in-service measurements on the propeller shaft by means of Monte Carlo simulations. A particular focus is on the sensitivity to the individual terms entering the STW model, which is necessary in order to identify the most critical parts, e.g. precision of the sensor measurements, model test data or external factors such as wind and waves. In the end, we conclude whether estimating STW from in-service measurements is reasonable, considering the expected uncertainties.

2. Case vessel

A general cargo/multipurpose vessel is used as a case vessel for the estimation of uncertainty in STW and directional sea current. The use of a case vessel provides better control over input to the analysis, as well as it provides results that is easier to evaluate in a physical manner. The vessel is designed by Kongsberg Maritime AS. It has an overall length of almost 120 m, beam and max draft of 20 m and 5 m respectively, and a dead weight of about 5000 dwt. The vessel is fitted with a rudder and a single screw controllable pitch propeller. The propeller has a diameter of $D = 4.2$ m, blade area ratio $A_E/A_0 = 0.515$ and a design pitch ratio of $P/D_{0.7} = 0.975$. The typical service speed of the vessel is about 15 knots.

The vessel is equipped with an in-service monitoring system collecting sensor data from selected vessel equipment. The data acquisition system provides measurement data to the data logger, which is configured to sample at a frequency of 1 Hz. The case vessel is, amongst other things, equipped with a NORSUB 4000 Motion Reference Unit (MRU), VAF Instruments TT-sense thrust and torque sensor, Furuno DS-60 Doppler Speed Log and a Furuno GP-150 GPS Navigator.

3. Uncertainty in STW

3.1. Estimating STW using propeller data

The speed through water can be estimated from propulsion related data such as propeller revolutions per minute (rpm), torque and/or thrust. The method was probably first described by Telfer (1927). In this paper, the method for estimating STW from propeller data is referred to as the STW model. A flow chart is given in Fig. 1 to illustrate the steps in the STW model.

There are various methods for measuring rpm, thrust and torque, but most involve the use of either strain gauges or optical sensors, or a combination of both. For ships prepared for in-service monitoring, it is quite common to install sensors on the propeller shaft. Measuring propeller rpm and torque is the most common, while including measurements of propeller thrust is still quite exceptional. This is naturally a matter of installation costs, however, the physical properties of the propeller shaft makes it far more challenging to get accurate measurements of propeller thrust as compared to propeller torque. For the sake of modeling STW from propeller data while ensuring that the procedure is generic, it is most convenient to assume that only rpm and torque is measured on the propeller shaft. The main part of the STW model is therefore based on using rpm and torque measurements on the propeller shaft. Considering the advances in sensor developments, it is however an interesting question whether the uncertainty in the STW estimate can be reduced by incorporating thrust measurements into the model. Various ways of including propeller thrust measurements in STW estimation is therefore presented and discussed in Section 3.4. As is the significance of including propeller thrust measurements in the STW estimation.

The performance of a propeller can be expressed through the dimensionless thrust K_T (1) and torque K_Q (2) coefficients. For a ship equipped with sensors measuring rpm, torque and/or thrust, the speed of water through the propeller V_a can be estimated directly through either K_T or K_Q in combination with the advance number J (3) as well as knowledge of the propeller characteristics (open water diagram).

$$K_T(J) = \frac{T}{\rho n^2 D^4} \tag{1}$$

$$K_Q(J) = \frac{Q}{\rho n^2 D^5} \tag{2}$$

$$J = \frac{V_a}{nD} \tag{3}$$

Considering that torque and propeller rpm is measured on the propeller shaft, the torque coefficient is calculated according to Eq. (2). The value of K_Q is used to find the propeller operating point J by intersecting K_Q on the $K_Q(J)$ curve. From the intersected J-value, the speed of water through the propeller V_a is calculated using Eq. (3). V_a is often referred to as advance speed.

For most practical applications however, V_a is less than the speed through water V. The difference in speed is expressed through the wake fraction w_s, see Eq. (4). For a single-screw vessel, the mean wake factor is typically around $0.2 - 0.3$ (Pecoraro et al., 2015), with a very modest increase with forward speed. When estimating STW from measurements on the propeller shaft, it is therefore essential that a suitable wake fraction is included in the hydrodynamic model. The traditional approach for full scale wake estimation is to scale the model scale wake fraction, obtained from the propulsion test and open water test, using a suitable scaling procedure. For single screw vessels, the propeller operates largely within the boundary layer from the hull for which the ITTC wake scaling procedure (ITTC, 2017a), reproduced in Eq. (5), is frequently used. In the scaling, t is the thrust deduction factor which can be calculated from the resistance and the propulsion test and w_m is the effective model scale wake fraction. C_{FS} and ΔC_F is the full scale frictional resistance coefficient and roughness correction, respectively, while C_{FM} is the model scale frictional resistance coefficient. For twin screw vessels there is no established practice for wake scaling, which in practice often means that the full scale wake is set equal to the model scale wake.

$$V_a = (1 - w_s)V \tag{4}$$

$$w_e = (t + 0.04) + (w_m - t - 0.04)\frac{C_{FS} + \Delta C_F}{C_{FM}} \tag{5}$$

The $K_Q(J)$ curve is usually established in the open water test by using a scaled model of the propeller. Occasionally, computational fluid dynamics (CFD) is used to establish the $K_Q(J)$ relation. The model scale wake fraction can be found by intersecting K_T from the propulsion test with the open water $K_T(J)$ curve, referred to as thrust identity. Nevertheless, the wake fraction is generally valid in the design condition only, which for all practical purposes means calm waters and straight ahead forward speed. Wake data in off-design conditions such as waves are rarely available, although it is known that the wake fraction in general is quite dependent on waves and ship motions (Nakamura and Naito, 1975; Guo et al., 2012; Sadat-Hosseini et al., 2013; Ueno et al., 2013; Taskar et al., 2016).

Taskar et al. (2016) presented a formula for the time varying total wake velocity in waves considering a mean increase in wake from the pitch motion, based on Faltinsen et al. (1980), as well as a fluctuating part caused by wave induced particle motion and vessel surging, based on Ueno et al. (2013). For the sake of estimating STW from propeller data, the use of a temporal resolution that evaluates the fluctuating part involving instantaneous particle motion and wave excitations is considered unnecessarily complicated. The STW model only considers the mean increase in the wake fraction w_{η_5} as given in Eq. (6) for the calculation of wake velocity in waves. The forward speed U in the equation should be the low-pass filtered surge speed, for which the instantaneous surge motions in waves are filtered out. The total effective full scale wake fraction in presence of waves is therefore expressed as $w_s = w_e + w_{\eta_5}$ in the STW model.

The mean increase in wake is built on potential flow theory and depends on the encounter frequency ω_e, the pitch amplitude $|\eta_5|$ and the longitudinal distance x from the center of gravity of the ship to the propeller. If the ship is equipped with a MRU or an inertial measurement unit (IMU), the encounter frequency can be obtained close to real time from the pitch motion. By further assuming the pitch motion to be approximately sinusoidal, the amplitude $|\eta_5|$ can be approximated from the standard deviation of the pitch motion, following Eq. (9). The case vessel used as reference in this paper has a six degrees of freedom MRU installed.

For other ships lacking equipment for ship motion measurements, a real time evaluation of the mean increase in wake fraction is not feasible. In such cases, the mean increase in wake fraction should either be completely disregarded or the estimation of STW must rather be based on post-processing the data. Disregarding the increase in wake fraction might however give an estimation bias in the STW. This will be further discussed in Section 3.4. During data post-processing, the mean increase in wake can be calculated based on hindcast wave data, for which the encounter frequency is calculated from the wave frequency ω and the wave encounter angle β according to Eq. (8). The pitch amplitude $|\eta_5|$ can be estimated from the pitch RAO obtained from e.g. linear strip theory calculations, from model experiments or by CFD.

Due to the speed dependency in wake fraction, the STW estimated from Eq. (4), should be solved by iteration. In terms of calculation performance, an initial condition should preferably be given to the full scale wake fraction, for instance, $w_s = 0.2$. For each estimate of STW (V), a new full scale wake fraction is found, and the iteration continues until the change in wake fraction is considered negligible.

$K_Q(J)$ relates to a given propeller pitch angle (α). If the propeller has controllable pitch, K_Q is rather a function of both J and α, i.e. changing with the propeller pitch angle. A set of pitch angles can be tested using CFD or with the scaled propeller model. In order to simplify the uncertainty analysis, it is however presumed that the STW estimation is active for 100% propeller pitch only. For the case vessel, this practically includes all standard transit operations, as the propeller usually operates at 100% pitch during transit. What nevertheless adds uncertainty to the STW estimation is whether the 100% full scale propeller pitch physically corresponds to the 100% model scale propeller pitch. Experience shows that a small bias between 100% propeller pitch on the vessel compared to the propeller design can be introduced during the propulsion system configuration. How this can be modeled in terms of adding uncertainty to the STW estimation is further elaborated in Section 3.2.6.

The STW model can be summarized with these steps, referring to the flow chart in Fig. 1:

1. Calculate K_Q from measured torque and rpm on the propeller shaft, based on Eq. (2).
2. Intersect the K_Q-value on the open water $K_Q(J)$-curve to find the advance number J.
3. Calculate the speed of water through the propeller V_a using Eq. (3).
4. Assume a total wake fraction w_s.
5. Find the estimated STW by Eq. (4).
6. Find the total wake fraction w_s as the sum of the following:
   (a) Full-scale wake fraction w_e.
   (b) Change in wake fraction due to vessel pitching in waves w_{η_5} following Eq. (6).
7. Iterate on step 5 and 6 until w_s has converged.
8. Calculate the final estimated STW from Eq. (4).

$$w_{\eta_5} = 1 - \sqrt{\left(1 - \frac{\Delta\overline{p}}{0.5\rho U^2}\right)} \tag{6}$$

where

$$\Delta\overline{p} \sim -\frac{\rho}{4}\omega_e^2|\eta_5|^2x^2 \tag{7}$$

$$\omega_e = \omega\left(1 - V\frac{\omega}{g}\cos\beta\right) \tag{8}$$

$$|\eta_5| = \sqrt{2}\sigma_{\eta_5} \tag{9}$$

3.2. Input uncertainties to the STW model

The uncertainty in the estimated STW is considered key knowledge in terms of deciding whether the STW model approach to speed determination might increase the overall accuracy of STW data from ships. Errors in the estimated STW is formed by the uncertainties in the input to the model, as well as errors in the modeling assumptions. In the following sections, each individual input will be thoroughly discussed, using the case vessel as a reference. The focus is to provide a knowledge base relevant for assigning values to each input uncertainty.

It is assumed that all uncertainties are zero mean gaussian processes, and that all input uncertainties are uncorrelated. This is a non-conservative assumption, which will be discussed. Each individual input uncertainty forms the parameters of the gaussian processes that is used to construct samples for simulating the STW model. The parameters of the gaussian processes are given consecutively in the next sections, and summarized in Table 8.

3.2.1. Propeller shaft measurements

The case vessel is single screw where thrust, torque and rpm is measured on the shaft. The STW model is however initially based on the propeller shaft torque and rpm measurements only. The uncertainty in thrust measurements is yet to be discussed, for evaluating the outcomes of incorporating thrust measurements into the STW model. The VAF TT-sensor specification states the sensor accuracy of thrust, torque and rpm measurements as given in Table 2 (error supplied). The reference is to full scale deflection (FSD), which means that the relative measurement accuracy is inverse to the loading.

No data for the particular installation of the shaft sensor is available. The value of FSD is therefore set based on the maximum loading of the main engine. The main engine delivers approximately 4000 kW with a maximum of 750 rpm. With a gear ratio of 5.25, this means that the torque sensor will measure approximately 260 kN m at maximum loading. The FSD is therefore assumed corresponding to 2×260 kN m = 520 kN m, which means an error of $< 0.25\cdot10^{-2}\times520$ kN m = 1.3 kN m.

Full scale resistance at the design speed and design draft corresponds to approximately 250 kN. The thrust sensor FSD is therefore assumed corresponding to 2×250 kN = 500 kN, which means an error of $< 1.00\cdot10^{-2}\times500$ kN = 5 kN.

For the rpm sensor the FSD is set equal to the maximum propeller shaft rpm. This equals 750/5.25 rpm $\approx$ 143, which means an error of $< 0.25\cdot10^{-2}\times143$ rpm = 0.4 rpm.

The propeller shaft measurement uncertainty distributions are based on the assumed measurement errors. The sample gaussian distributions of thrust, torque and rpm is therefore $\mathcal{N}(T,5)$ for the shaft thrust, $\mathcal{N}(Q,1.3)$ for the shaft torque and $\mathcal{N}(n,0.4)$ for the propeller rotational speed.

3.2.2. Ship motions

Ship motion measurements in terms of pitch amplitude $|\eta_5|$ and encounter frequency ω_e are used to estimate the mean increase in wake fraction due to waves. Encounter frequency is not a measurement in itself, but can be calculated from the pitch motion measurement by analyzing its frequency content. For small waves not capable of exciting vessel pitch motions, the encounter frequency analysis will not be feasible. Yet, there is in this case no need for the encounter frequency, as the increase in wake fraction is caused by the pitching motion.

The case vessel is equipped with a NORSUB 4000 MRU measuring the pitch motion. The sensor accuracy supplied by the manufacturer is given in Table 3. It is assumed that the error in the pitch angle measurement is normally distributed around the measurement value. This basically means that the measurement is assumed to be unbiased. The standard deviation of the normal distribution is approximated to 1/4 of the supplied error, which means that 95% of the pitch measurements are assumed to be covered by the accuracy limits supplied

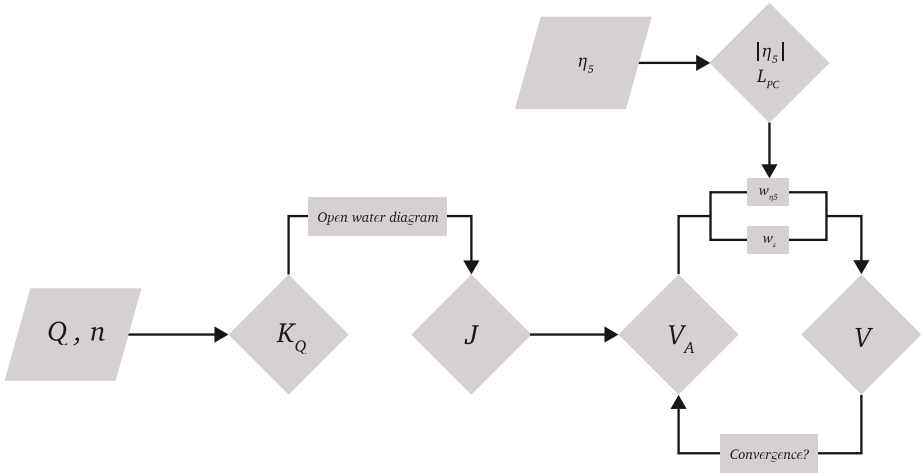

Fig. 1. Flow chart presentation of the STW model.

Table 1
Notations used in the paper.

Symbol	
CP, FP	Controllable pitch, Fixed pitch
MRU, IMU	Motion Reference Unit, Intertial Measurement Unit
STW, SOG	Speed Through Water, Speed Over Ground
FSD	Full scale deflection
COB	Center of buoyancy
OAT	One at a time
Q	Torque measured on propeller shaft
T	Thrust measured on propeller shaft
n	Propeller rpm
D	Propeller diameter
ρ	Density of water
J	Advance number
K_Q	Torque coefficient
K_T	Thrust coefficient
V	Speed through water (STW)
V_a	Advance speed
w	Wake fraction
w_e	Full scale wake fraction in calm water
w_{η_5}	Mean increase in wake fraction due to vessel pitching
u_v	Longitudinal current speed
α	Propeller pitch angle at 70% radius
$_s$	Subscript used to indicate variable on ship
$_m$	Subscript used to indicate variable on model
L_{PC}	Length between propeller and center of buoyancy (COB)
L_{P2}	Length between propeller and $L_{PP}/2$
μ, σ	Mean value, Standard deviation
A_i	Local sensitivity coefficient of input factor i
K, S_{KP}	Excess kurtosis, Skewness
N	Monte Carlo sample size
k	Number of input factors in the STW model
X_i	Input factor i to the STW model
x_i^j	Sample value j of input factor i
Y	STW model output (scalar) equal to $Y = \phi(X_1, X_2, \ldots, X_k)$
U_i	Uncertainty of input factor i
$\mathbf{X}$	$N \times k$ matrix of input factors
$\mathbf{A}$, $\mathbf{B}$	$N \times k$ sample matrices of input factors
$\mathbf{X}_{\sim i}$	$N \times (k-1)$ matrix of all factors except X_i
$\mathbf{A}_{\mathbf{B}}^{(i)}$	Matrix $\mathbf{A}$ where column i is replaced by column i in matrix $\mathbf{B}$

Table 2
VAF TT-sense supplied and assumed sensor accuracy based on full scale deflection (FSD).

Measurement	Error supplied	Error assumed
Thrust	<1.00% FSD	<5 kN
Torque	<0.25% FSD	<1.3 kN m
RPM	<0.25% FSD	<0.4 rpm

Table 3
NORSUB 4000 MRU measurement accuracy supplied by the manufacturer.

Measurement	Error
Pitch	±0.05°

by the manufacturer. The resulting gaussian distribution of the pitch measurements becomes $\mathcal{N}(\eta_5, 0.02°)$, where η_5 is the instantaneous pitch angle measurement.

The pitch amplitude is calculated from the standard deviation of the pitch motion, following Eq. (9). The standard deviation of the pitch motion is based on a moving window, which ensures sufficient timing between the mean increase in wake fraction and the particular STW estimation. The window size is set to 1 min, or 60 samples, considering that the in-service monitoring system samples at 1 Hz.

The encounter frequency is estimated from the same moving window as the pitch amplitude, by running a Fast Fourier Transform (FFT) of the signal. No additional uncertainty is added to the encounter frequency, which means that the uncertainty in the encounter frequency estimation is directly linked to the uncertainty in the pitch motion measurements.

3.2.3. Model test data

The STW estimation is based on using model test data for estimating wake fraction w_m and the open water curve $K_Q(J)$. In the open water test, $K_Q(J)$ is calculated from measured shaft moment, shaft frequency and forward speed following Eqs. (2) and (3). The measurements in the open water test are uncertain, which means that $K_Q(J)$ is based on uncertain measurements. Additionally comes the uncertainty in the propeller geometry and the water density during the test, the latter mainly a result of uncertainty in water temperature. In total, the $K_Q(J)$ curve has inherent uncertainty that has to be considered when being used for estimating the STW.

The uncertainty in $K_Q(J)$ caused by the uncertainty in shaft moment, rotational speed and forward speed can be estimated from repeated open water test measurements. For single runs already completed, there is however no direct approach for estimating the uncertainty in $K_Q(J)$. There is also missing information regarding the accuracy of the water temperature measurement during the open water test, as well as the uncertainty in propeller geometry. The model scale propeller for the specific case vessel is however manufactured to be geometrically similar to the actual full scale propeller. The uncertainty in geometry is therefore only related to inaccuracies in production.

Considering the unavailable information, the uncertainty in $K_Q(J)$ is rather based on the work published by ITTC (2014b). ITTC separates

Table 4
ITTC open water test relative bias and precision limits.

Variable	Bias+precision limit
K_T	0.730%
K_Q	0.850%

Table 5
ITTC propulsion test relative speed and wake bias and precision limits.

Variable	Bias+precision limit
w_m	2.3335%

the elementary error sources into calibration, data acquisition, data reduction and conceptual bias. The uncertainty parameters that are used from this work are given in Table 4, specific for an advance number of $J = 0.6$.

The open water test curve $K_Q(J)$ is used to determine the operational advance number J based on the operational torque coefficient K_Q (calculated using Eq. (2)). Uncertainty in the open water test gives uncertainty to the $K_Q(J)$ curve, that propagates through J to the estimated STW. It is assumed that the measurements in the open water test have constant uncertainty along the entire measurement range, which means that it is rather the relative uncertainty that changes along the measurement range. With reference to the ITTC work (ITTC, 2014b), $K_Q(J = 0.6)$ is used as a basis for setting the input uncertainty. It should also be noted that $J = 0.6$ represents a typical advance number for the case vessel. Similar as for the other input factors, it is assumed that the errors are gaussian distributed around the measurement values. For $K_Q(J)$ this implies that each point along the curve is gaussian distributed with its specific mean and a constant standard deviation. This gives the input distributions $\mathcal{N}\left(K_T(J), K_T|_{J=0.6} \cdot (0.73/100)\right)$ for the K_T values and $\mathcal{N}\left(K_Q(J), K_Q|_{J=0.6} \cdot (0.85/100)\right)$ for the K_Q values. The specific values of $K_T|_{J=0.6}$ and $K_Q|_{J=0.6}$ are not given for reasons of confidentiality.

The wake fraction w is used to calculate speed through water from the speed through the propeller, following Eq. (4). Based on model scale experiments, the model scale wake fraction w_m is found by relating the open water test advance number J_0 to the corresponding advance number in the propulsion test. The wake fraction is usually given as a constant value, or a speed dependent curve $w_m(V)$. Because the measurements in the open water test and the propulsion test are uncertain, the wake fraction is also uncertain, which should be taken into consideration when estimating the STW.

The uncertainty in $w_m(V)$ follows a similar reasoning as for $K_Q(J)$, which implies that there is no direct approach for estimating the uncertainty in $w_m(V)$ based on single runs. The uncertainty in $w_m(V)$ is therefore based on ITTC (2017b), summarized in Table 5. The uncertainty is specific for a Froude number of $F_N = 0.21$.

Uncertainty in the open water test and propulsion test gives uncertainty to the $w_m(V)$ data, that propagates to the estimated STW. As for the open water test, it is assumed that the measurements in the propulsion test have constant uncertainty along the entire measurement range. With reference to the ITTC work (ITTC, 2017b), $w_m(V|_{F_N=0.21})$ is used as a basis for setting the input uncertainty. $V|_{F_N=0.21}$ refers to the ship speed corresponding to $F_N = 0.21$, which is not given for reasons of confidentiality. It is further assumed that the errors are gaussian distributed around the measurement values. For $w_m(V)$ this implies that each point along the curve is gaussian distributed with its specific mean and a constant standard deviation. This gives the input distribution $\mathcal{N}\left(w_m(V), w_m(V|_{F_N=0.21}) \cdot \frac{2.3335}{100}\right)$.

The ITTC wake scaling procedure is used to estimate the full scale effective calm water wake fraction w_e based on the model scale wake fraction, see Eq. (5). The wake scaling has certainly a contribution to the uncertainty in the estimated STW. However, the process of quantifying the uncertainty in the wake scaling is challenging. Including such uncertainty, without having confidence in whether or not the uncertainty parameters in fact are representative for the wake scaling, is therefore considered to be less useful in terms of interpreting the final uncertainty in STW. The uncertainty in wake scaling is therefore left to be discussed in the evaluation of the total uncertainty in estimated STW.

3.2.4. Ship parameters

Among the inputs to the STW model, two variables are referred to as ship parameters. These are the propeller diameter D and the longitudinal distance from the propeller to the center of buoyancy (COB), referred to as the distance L_{PC}. It is assumed that the full scale propeller is geometrically similar to the model scale propeller. Total similarity is however not possible due to machining tolerances in production, which will add uncertainty to the STW estimation. The only input to the STW model concerning propeller geometry is the propeller diameter. ITTC (2002) assumes the error in the model diameter to be within ± 0.1 mm, corresponding to 0.044% of the nominal diameter. Full scale inaccuracies are expected to be larger. ISO (1981) machining tolerances relevant for the case vessel (Class I) refers to a precision of $\pm 0.15\%$ of the propeller diameter. This has been assumed for the full scale production in the current study. The sampling of the propeller diameter is therefore assumed to follow the gaussian distribution $\mathcal{N}\left(4.2, 6.3 \cdot 10^{-3}\right)$. Note that the uncertainty in propeller diameter should be considered a bias factor, and is not related to any variable that is measured onboard the ship. The STW model can be tuned to overcome this bias factor by a physical end-to-end calibration, which also removes the other uncertainties concerning propeller geometry. This will be further discussed in Section 3.4.

Regarding the position of the propeller, it is assumed that the physical position is fixed relative to the hull. The distance L_{PC} from the propeller to the COB might however vary, due to a variation in COB with the fore/aft draft. It is therefore assumed that the total uncertainty in L_{PC} is gathered in the uncertainty in COB.

The COB can be determined by combining draft measurements with displacement data. Traditional draft sensor technology is based on pressure tubes located fore and aft. This is a simple technique, however not very reliable. Pressure tubes are usually sensitive to waves, which at minimum will require the use of a low pass filter. The draft readings are however also affected by the forward speed of the vessel. It is therefore recommended that draft data is extracted prior to starting a transit operation, when the ship moves slowly and operates in sheltered waters (Dalheim and Steen, 2020).

The case vessel is equipped with pressure tubes measuring draft fore and aft. By forming a parametric relation between draft and COB, the draft measurements can be used directly to estimate COB, and moreover, the uncertainty in draft measurements can be propagated to form the uncertainty in the COB. The parametric relation is assumed to be linear for the case vessel, which means that it can be established based on two sailing conditions, i.e. data from two distinct waterlines. The draft conditions are referred to as WL1 and WL2, and are assumed to define the range in which the COB varies. It is further assumed that the COB is gaussian distributed around the center of this range and with a standard deviation equal to 1/4 of the range. This means that 95% of the COB data will be covered by the selected draft conditions. The case vessel COB data is given in Table 6, where the distance relates to the center between the perpendiculars ($L_{PP}/2$). The resulting parameters for the distribution of L_{PC} becomes $\mathcal{N}(L_{P2} - 5.0845, 0.02725)$, where L_{P2} is the distance from $L_{PP}/2$ to the propeller.

3.2.5. Environmental parameters

The water density ρ enters the STW model in the calculation of $K_Q(J)$. In general, ρ depends on water temperature t_w and salinity S_w. The International Association for the Properties of Water and Steam (IAPWS) has developed equations expressing water properties such as water density (IAPWS, 2008). This has been used as a reference to

Table 6
Center of buoyancy (COB) in meters relative to the center between the perpendiculars ($L_{PP}/2$) at two water lines for the case vessel.

Water line	COB [m]
WL1	−5.030
WL2	−5.139

Table 7
Input values to the uncertainty in water density ρ.

Input	Value
U_x	10^{-4}
$\partial\rho/\partial t_w$	−0.1710
$\partial\rho/\partial S_w$	0.7670

express the input uncertainty U_ρ to the STW model, as given in Eq. (10). The total uncertainty in ρ depends on the inherent uncertainty in the IAPWS-equation (U_x), uncertainty in temperature (U_{t_w}) and uncertainty in salinity(U_{S_w}). Input values to Eq. (10) are given in Table 7 for a nominal temperature of $t_w = 15°$ and salinity of $S_w = 35‰$.

$$U_\rho = \sqrt{(U_x)^2 + \left(\frac{\partial\rho}{\partial t}U_{t_w}\right)^2 + \left(\frac{\partial\rho}{\partial S}U_{S_w}\right)^2} \tag{10}$$

From IOC et al. (2010), the estimated uncertainty in standard absolute salinity is $U_{S_w} = \pm 0.007$ g/kg. Details about the case vessel temperature sensor, and its precision limits specifically, were not available. It is therefore assumed that the uncertainty in the measured temperature is equal to $U_{t_w} = \pm 0.3$ °C, which is based on a DNV-GL approved type of screw-in temperature sensor (TP8) by Noris Group GmbH (NORIS Automation GmbH, 2015). This is also between the two uncertainties used by ITTC (2011) in the example calculation of uncertainty estimates for saltwater properties. In total, this gives $U_\rho = 0.0516$, which is used as the standard deviation of the water density. Assuming a nominal temperature of $t_w = 15$ °C, this gives the gaussian distribution $\mathcal{N}(1026.021, 0.0516)$ as input distribution for ρ to the STW model.

3.2.6. Propeller pitch angle

As previously mentioned, the case vessel has a controllable pitch propeller, which means that $K_Q(J)$ relates to a given propeller pitch angle (α). The propeller (model scale) has only been tested at 100% pitch, referred to as design pitch. As practically all standard transit operations for this case vessel are operated close to 100% pitch, the uncertainty analysis of the STW model has been simplified in terms of only taking the $K_Q(J)$-curve representing design pitch into consideration.

There is however some uncertainty that should be added to the STW estimation. Experience shows that the geometrical 100% full scale propeller pitch not always corresponds to the 100% model scale propeller pitch. This bias is usually introduced during the propulsion system configuration, when the geometrical position of 100% pitch is adjusted. As the propeller is usually fully submerged during this configuration, it is challenging to physically measure the geometrical propeller angle. Not to mention to obtain measurements with high accuracy.

There is no straightforward method of setting the pitch angle bias limit. A precise estimation requires access to a large number of propeller configurations, for which the geometrical propeller pitch angles in model- and full scale can be compared. This has not been attainable, which has forced another approach. The uncertainty in K_Q caused by the propeller pitch angle α is referred to as $U_{K_{Q,\alpha}}$ and is the product of the sensitivity in $K_Q(\alpha)$ referred to as $\frac{\partial K_Q}{\partial\alpha}$ and the bias in α, referred to as U_α. This is expressed mathematically in Eq. (11). $\partial K_Q/\partial\alpha$ is preferably established based on testing the propeller for a number of pitch angles. In the present study, $\partial K_Q/\partial\alpha$ is rather estimated from standard Wageningen B-series (Bernitsas et al., 1981) propellers of similar geometry, by looking at the change in K_Q (ΔK_Q) relative to $\Delta\alpha$, see Eq. (11). Values for a 4-bladed propeller with blade area ratio $A_E/A_0 = 0.515$ were used. More specifically, the change in K_Q was calculated for $J = 0.6$ and pitch ratios $P/D \in \{0.9745, 0.9746 \ldots 0.9755\}$. The resulting sensitivity parameter was found to be $\partial K_Q/\partial\alpha \approx 0.3213$.

Table 8
Summary of the input parameter distributions (gaussian) used to estimate uncertainty in the STW model.

X_i	$\mathcal{N}(x_i^0, \sigma_{x_i})$
Q	$\mathcal{N}(Q, 1.3)$
n	$\mathcal{N}(n, 0.4)$
ρ	$\mathcal{N}(1026.021, 0.0516)$
D	$\mathcal{N}(4.2, 6.3 \cdot 10^{-3})$
K_Q	$\mathcal{N}(K_Q(J), K_Q\|_{J=0.6} \cdot (0.85/100))$
w	$\mathcal{N}(w_m(V), w_m(V\|_{F_N=0.21}) \cdot (2.3335/100))$
η_5	$\mathcal{N}(\eta_5, 0.025)$
L_{PC}	$\mathcal{N}(L_{P2} - 5.0845, 0.02725)$
$\Delta K_{Q,\alpha}$	$\mathcal{N}(0, 9.669 \cdot 10^{-4})$

$$U_{K_{Q,\alpha}} = \frac{\partial K_Q}{\partial\alpha}U_\alpha \tag{11}$$

$$\frac{\partial K_Q}{\partial\alpha} \approx \frac{\Delta K_Q|_{J=0.6}}{\Delta\alpha} \tag{12}$$

U_α in Eq. (11) refers to the bias limit in the geometrical propeller pitch angle corresponding to 100% pitch. As it has not been attainable to quantify U_α from actual data, it is rather assumed that the propeller pitch follows a gaussian distribution centered at the design pitch with a standard deviation of $\sigma_\alpha = 3\text{x}10^{-3}$ [rad] (1%). In terms of the change in K_Q caused by the uncertainty in α (referred to as $\Delta K_{Q,\alpha}$), this standard deviation is mapped through Eq. (11) to the gaussian distribution $\Delta K_{Q,\alpha} \in \mathcal{N}(0, 9.669 \cdot 10^{-4})$.

3.2.7. Input uncertainty summarized

All input parameters that are considered to be uncertain are assumed to be gaussian distributed around its respective nominal value, with a standard deviation in order of magnitude relative to the expected uncertainty in the parameter. The reasoning behind the resulting input uncertainties have been presented in the previous sections. In Table 8, the distributions of the input parameters are summarized.

The input uncertainties to the STW model are basically independent of the forward speed of the vessel, except for the uncertainty in K_Q and w that relates to a particular advance number and Froude number, respectively. Changes in forward speed will however cause only minor changes in the operating advance number, suggesting that the uncertainty in K_Q might also be considered independent of the forward speed. A similar reasoning can be used for the wake fraction that will not change very much with the forward speed, which means that the uncertainty in w can be considered independent of the forward speed.

3.3. Sensitivity analysis

Sensitivity analysis correspond to a set of statistical methods that examine how a model reacts to a change in its input factors. The overall goal is to measure how variations propagate from the input factors to the output, i.e. describing the relative importance of each input in determining the output (Saltelli et al., 2007). The input factor sensitivity can be analyzed at a local or global level. The local methods investigate the effect of varying an input around a given point in the input space, using the one factor at a time method (OAT). Global methods allow concurrent input variation in the complete input space, and decompose the overall output variance into contributions from the different input factors. The following sections investigate the local and global sensitivity indices of the input factors to the STW model. The input to the sensitivity analyses are based on the specifications in Table 8. As the nominal operating point, the values of $Q = 150$ and $n = 108$ have been used, which represent a typical operating point for the case vessel.

Table 9
Convergence study of required number of Monte Carlo simulations (N) in order to obtain a stable standard deviation of estimated STW (σ_{STW}). The right column shows the change in the standard deviation of estimated STW ($\Delta\sigma_{STW}$) when N is increased according to the left column.

N (from → to)	$\Delta\sigma_{STW}$
1 000 → 5 000	4.2%
5 000 → 10 000	1.1%
10 000 → 30 000	0.2%

Table 10
Local sensitivity coefficients of all input factors to the STW model, as well as goodness of fit (R^2) to linear model. Monte Carlo simulation (N = 10 000) with OAT factor variation. Assuming no waves.

X_i	A_i	R^2
Q	−0.9999	0.9999
n	0.9999	0.9998
ρ	1.00	1.00
D	1.00	0.9999
K_Q	0.9810	0.9624
w	0.9999	0.9999
α	−0.9976	0.9952

3.3.1. Local sensitivity

The local sensitivity analysis investigates how a small perturbation around the input space value $\mathrm{x}^0 = (x_1^0, x_2^0, x_3^0, \ldots, x_k^0)$ influences the output value y of the STW model $y = \phi(x^0)$ for input factors $1 \ldots k$. It consists of estimating

$$A_i = \left.\frac{\partial y}{\partial x_i}\right|_{\mathrm{x}^0=(x_1^0,\ldots,x_k^0)} \tag{13}$$

that characterizes the effect on the estimated STW (y) caused by a perturbation of the input X_i near a nominal value x_i^0. The local sensitivity coefficients A_i are formally defined as first-order partial derivatives of the model output with respect to the input factor X_i. In this study, the partial derivatives are not analytically available, and they are therefore approximated through Monte Carlo simulations and the classical OAT approach. That is, each input factor $i \in \{1 \ldots k\}$ is sampled from its probability distribution while the other $k-1$ input factors are fixed at their respective nominal values.

The local sensitivity coefficients are determined by simple linear regression on the STW model response using the ordinary least squares method. It is assumed that the influence is approximately linear for all input variables, which means that each local sensitivity coefficient is given by the linear regression slope coefficient β_i. In fact, standardized regression coefficients are used such that the sensitivity coefficients can be compared relative to each other. The standardization follows Eq. (14), where σ_x and σ_y represent the estimated standard deviations of the input and the output, respectively. In order to assess the goodness of fit to the linear model, the R^2 statistics is also calculated. A series of Monte Carlo simulations (N = 10 000) are run to estimate the local sensitivity coefficients. The selection of N is based on a convergence study, given in Table 9. The perturbations around the nominal values are based on the respective uncertainties of the input factors. The result of the local sensitivity analysis is given in Table 10.

$$\beta^* = \beta\frac{\sigma_x}{\sigma_y} \tag{14}$$

The local sensitivity coefficients are established by connecting the output to the input. For the coefficients A_{K_Q} and A_w this is however not straightforward, as K_Q and w are functions of J and V, respectively. $K_Q(J)$ consists of K_Q-values for all the advance numbers tested in the open water test, while $w(V)$ consist of wake fractions for all forward speeds tested in the resistance and propulsion test. When adding uncertainty to K_Q and w, this means that a set of values are allowed to vary, while the result is still just a single output. In other words, for each sample in the Monte Carlo simulation, multiple values ($K_Q(J)$ or $w(V)$) are supposed to be mapped to one single output (STW) through the sensitivity coefficient, but this is not achievable. In the analysis of the two local sensitivity coefficients A_{K_Q} and A_w, the coefficients are rather based on mapping the average perturbation of $K_Q(J)$ and $w(V)$ to the output variation in the STW. A number of strategies are conceivable to construct this average perturbation. If polynomial curves are fitted to the K_Q and w data, the average perturbation has to consider the uncertainty in all of the data points. The result of this is shown in Fig. 2 for the K_Q data for a subset of advance numbers. The perturbations in K_Q, i.e. the uncertainty, is shown along the first axis, while the resulting perturbation in STW is shown on the second axis. Each curve represent data for the given J-value, and the slope is therefore to be considered as the local sensitivity to K_Q when K_Q is uncertain at that particular J-value. What is evident from this figure, is that the local influence coefficient is depending on for what J-value the uncertainty is included. Adding uncertainty to data that is more at the center of the J-values has a very different effect on the resulting STW as compared to uncertainty added to the lower and higher regions of the J-values. Defining an average resulting perturbation based on all the $K_Q(J)$ data is therefore not considered practical, not to mention reasonable. The chosen strategy is therefore rather to form the average perturbation based on allowing only the two K_Q values closest to the full scale operating point to be uncertain, and perform a linear interpolation between the two nearest K_Q-values instead of including all K_Q-values in a polynomial fit.

For the wake data, the strategy is somewhat different. Based on model test results, it is assumed that the wake fraction is linear to the forward speed. The resulting perturbations in STW caused by uncertainty in w is shown in Fig. 3, similar to the K_Q-data. Because $w(V)$ is assumed linear, the local sensitivity coefficients behave different from the local sensitivity coefficients of $K_Q(J)$, which implies that A_w can be established by mapping the average perturbation of $w(V)$ to the output variation in the STW, based on the complete set of $w(V)$ data.

All of the local sensitivity coefficients, except for A_{K_Q} and A_α, are found to be close to one. This means that the input standard deviation maps to the standard deviation in STW in a one-to-one relation, with positive or negative signs. The estimated R^2 also shows that these sensitivity coefficients are virtually constant. The local sensitivity of K_Q is however less that one, which means that the input standard deviation of K_Q in the open water test is reduced in the curve fit to a lower output standard deviation. This seems reasonable as the local sensitivity of K_Q is based on averaging the perturbations of the two K_Q values enclosing the operating torque coefficient. The local sensitivity of the propeller pitch angle α is also found to be less than one. This is also reasonable, as the uncertainty in α maps through the K_Q curve. It is therefore concluded that all of the input factors are linear to the STW output.

3.3.2. Global sensitivity of the input factors

The global sensitivity of the input factors is explored using a variance-based global sensitivity analysis. This type of analysis studies how uncertainty in the output of the STW model can be apportioned to different sources of uncertainty in the model input factors. Variance based methods have a long history in sensitivity analysis. The work of Sobol (1993) is however considered a milestone. The total sensitivity indices that have been used were proposed in Jansen et al. (1994), and further discussed in Homma and Saltelli (1996).

Given a generic model $Y = f(X_1, X_2, \ldots, X_k)$, the variance based first order effect for a generic factor X_i can be expressed as (see the notations on Table 1):

$$V_{X_i}(E_{\mathbf{X}_{\sim i}}(Y|X_i)) \tag{15}$$

X_i is the ith input factor and $\mathbf{X}_{\sim i}$ is the matrix of all input factors except for X_i. The associated sensitivity measure (first order sensitivity coefficient) is expressed as

$$S_i = \frac{V_{X_i}(E_{\mathbf{X}_{\sim i}}(Y|X_i))}{V(Y)} \tag{16}$$

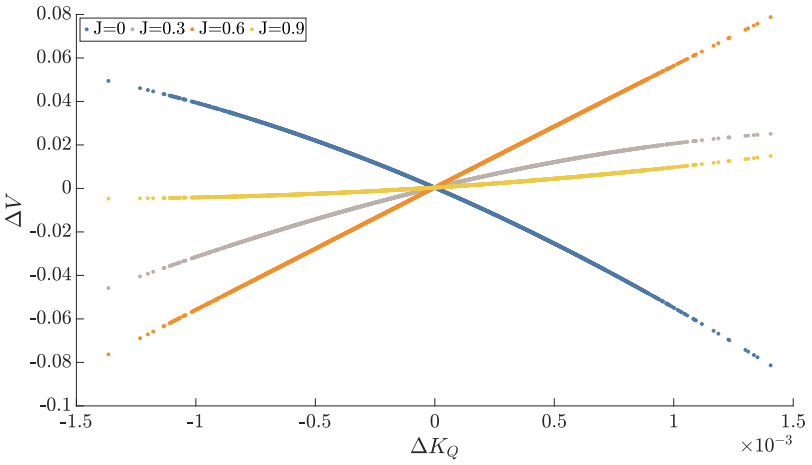

Fig. 2. Local sensitivity factor estimation of K_Q for a subset of advance numbers.

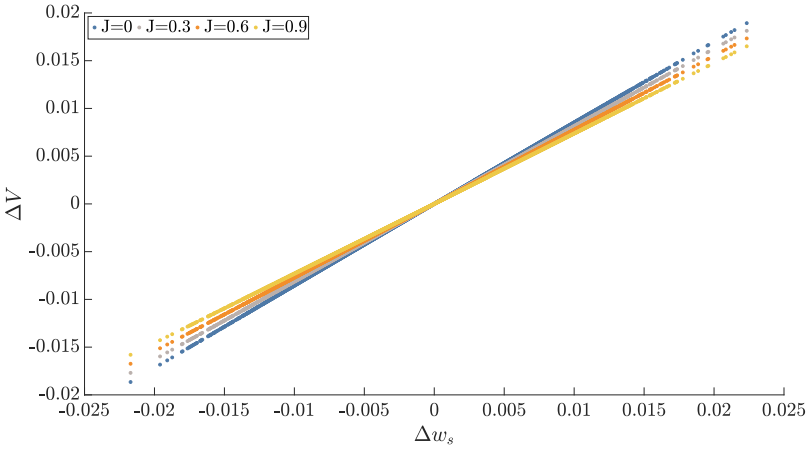

Fig. 3. Local sensitivity factor estimation of w_s for a subset of advance numbers.

where $V(Y)$ is the total variance in Y, given in Eq. (20). S_i is a normalized index, which means that the sensitivity coefficients can be compared between various input factors.

The second variance based measure that is useful is the total effect index S_{Ti}, expressed as:

$$S_{Ti} = \frac{E_{\mathbf{X}_{\sim i}}(V_{X_i}(Y|\mathbf{X}_{\sim i}))}{V(Y)} \tag{17}$$

S_{Ti} measures total effect, including higher order effects and interactions of input factor X_i. The equations decomposing this variance based framework are based on the suggestions by Saltelli et al. (2010) as expressed in Eqs. (18) to (20). In terms of the STW model, Y is to be considered as the estimated STW, while $f()$ consolidates all steps in the STW model. $\mathbf{A}$, $\mathbf{B}$ and $\mathbf{A_B}$ is the generated input data to the STW model, generated according to the notations in Table 1.

$$V_{X_i}(E_{\mathbf{X}_{\sim i}}(Y|X_i)) = V(Y) - \frac{1}{2N}\sum_{j=1}^{N}\left(f(\mathbf{B})_j - f(\mathbf{A}_\mathbf{B}^{(i)})_j\right)^2 \tag{18}$$

$$E_{\mathbf{X}_{\sim i}}(V_{X_i}(Y|\mathbf{X}_{\sim i})) = \frac{1}{2N}\sum_{j=1}^{N}\left(f(\mathbf{A})_j - f(\mathbf{A}_\mathbf{B}^{(i)})_j\right)^2 \tag{19}$$

$$V(Y) = \frac{1}{N}\sum_{j=1}^{N} f(\mathbf{A})^2 - \left(\frac{1}{N}\sum_{j=1}^{N} f(\mathbf{A})\right)^2 \tag{20}$$

The resulting first order and total effect indices are shown in Fig. 4 for the case vessel. The figure reveals that the uncertainty in the propeller pitch (K_{Q_α}) dominates the uncertainty in the estimated STW, with more than 71% of the total uncertainty in STW being described by the propeller pitch. Next, the uncertainty in propeller rpm is found to control almost 12% of the total uncertainty in STW. For the controllable pitch propeller, the detached uncertainty in STW based on uncertainty in the model test K_Q data (given that the propeller pitch is exact) is found to be small, while the uncertainty in model scale wake fraction and water density is found to be negligible.

Because the propeller pitch controls the total uncertainty in STW to such an extent, it is necessary to investigate the global sensitivity when keeping the propeller pitch fixed. That is, the uncertainty in full scale propeller pitch would never be zero, but zero uncertainty is still used to explore the global sensitivity of the remaining input factors to the STW model. The result for the fixed pitch propeller is shown Fig. 5. It is found that the propeller rpm has the largest contribution to the overall uncertainty in the estimated STW, with a dedication of more than 36% of the global uncertainty. Uncertainty in the propeller diameter and propeller torque follows with contributions of 22.8% and 22.3%, respectively. When the propeller pitch is fixed, the uncertainty in model test K_Q becomes more prominent, while the uncertainty in model wake fraction is still negligible in terms of the contribution to the global uncertainty.

Full scale measurements of propeller rpm are, in general, more precise compared to torque measurements. It is therefore worth noting that the uncertainty in propeller rpm contributes more to the overall uncertainty in STW than the uncertainty in propeller torque. It is not unlikely that the uncertainty in measured shaft rpm in fact can be lower than used in this analysis. At least one should expect the

Table 11
Resulting parameters of the STW model output for the case vessel.

	μ_V [knots]	σ_V [knots]	K_V	S_{KP}
CPP	12.3047	0.4499	0.08	−0.07
FPP	12.3039	0.2406	−0.09	−0.04

rpm measurement to be more stable than the torque measurement, particularly in terms of sensor drifting. Over time, this might result in the uncertainty in propeller rpm contributing less to the uncertainty in STW compared to the propeller torque.

3.4. Expected uncertainty when estimating STW using propeller data

The case vessel is Monte Carlo simulated ($N = 10\ 000$) using the STW model in order to establish the expected uncertainty in the estimated STW. Due to the significant impact from uncertainty in propeller pitch discovered during the sensitivity analysis, the vessel is simulated with both a CP and a FP propeller. The results are given in Table 11. The expected STW is estimated to 12.3 knots with a standard deviation of 0.45 knots, which corresponds to 3.7% of the estimated STW. By introducing a FP propeller, this uncertainty is reduced to 0.24 knots, or 1.96% of the estimated STW, which corresponds to a 53.5% reduction in total uncertainty. The significant reduction in STW uncertainty obtained by fixed propeller pitch angle is explained by the significant sensitivity index of $K_{Q\alpha}$, as shown in Fig. 4.

For both the CP and the FP propeller, the resulting STW is gaussian distributed with excess kurtosis (K_V) and skewness (S_{KP}) approximately zero. In terms of the expected uncertainty in estimated STW, the distributions have larger standard deviations compared to the Doppler speed log errors reported by Taudien and Bilen (2018). It should however be emphasized that Taudien and Bilen (2018) analyzed the various Doppler speed log configurations in a towing tank experiment, giving an experimental environment much easier to control. For Doppler instruments providing STW data on full scale ships, some of the basic assumptions of the Doppler principle are violated, such as the uniformity of the flow and the presence of acoustic noise pollution beneath the hull.

The Furuno DS-60 Doppler sonar mounted on the case vessel is stated to serve an accuracy of the water tracking speed equal to 1% or 0.1 knots, whichever is greater. At the chosen service condition of the case vessel, the accuracy of the DS-60 is therefore 1%. This is better than the standard deviation of STW obtained by the STW model, particularly if the ship is equipped with a CP propeller (3.7%), but also if the propeller is fixed pitch (1.96%). Based on experience in full scale data analysis of various ships, combined with the considerable amount of concerns in the literature related to the accuracy of speed logs, there are however reasons to believe that the precision limits supplied by the manufacturer are far too optimistic, meaning that full scale STW measurements in fact are more uncertain than what has been stated. This is basically a challenge concerning most kinds of sensor equipment, for which the precision limits supplied by the manufacturer are to be considered as the absolute lower limits of the sensor uncertainty. In real operating conditions, the given precision limits are usually impossible to fulfill. This motivates the use of STW estimation from propeller data. At the very least, the STW estimate could be used for validation of the speed log measurements from a continuous observation of the signal, giving notice if e.g. the speed log signal drifts or develops calibration issues. Or, the STW model could run in parallel to other STW measurements, such as the speed log, to produce a sort of best estimate from averaging the two STW values. As long as the two inputs have similar uncertainty, the average of the two will have lower uncertainty than each of the individual inputs. On the other hand, it is not unlikely that the individual STW model sensor accuracies can be further improved, without adding much extra cost to equipment and installation. This could certainly lead to STW estimation from propeller data becoming more attractive, particularly if the precision of sensors having large sensitivity indices such as propeller rpm and torque is improved.

Table 12
Additional input parameter distributions (gaussian) used to estimate uncertainty in the STW model when including thrust measurements.

X_i	$\mathcal{N}(x_i^0, \sigma_{x_i})$
T	$\mathcal{N}(T, 5)$
K_T	$\mathcal{N}\left(K_T(J), K_T\vert_{J=0.6} \cdot (0.73/100)\right)$
$\Delta K_{T,\alpha}$	$\mathcal{N}\left(0, 4.781 \cdot 10^{-3}\right)$

Similar to the traditional speed log, the STW model does not consider individual sensor calibration errors, which might introduce additional bias in the STW estimation. The most primitive way of avoiding calibration errors are by running a physical end-to-end calibration. Over a sufficient amount of time, the average SOG and STW should be equal. This however requires that no specific equipment for sailing optimization in terms of ocean current is installed. SOG is usually measured using high quality GPS sensors, that provide SOG with very high accuracy. In the end-to-end calibration, a total calibration factor can therefore be added to the STW model based on the difference in average SOG and STW over time.

3.4.1. Including thrust measurements

For sensor installations on ships also including measurements of propeller thrust, there are various ways of including these measurements in the STW model. One method is to use the thrust measurement solely, by equating the thrust T and thrust deduction t with the ship resistance R_T, as in Eq. (21), to find the ship speed from the speed dependent resistance. This method is only applicable in sailing conditions for which the ship resistance is known, which generally means calm water. If the sailing condition includes wind and/or waves, a number of corrections have to be made to the calm water resistance, as described in Dalheim and Steen (2020). Such corrections will introduce additional uncertainty to the STW estimation, that is expected to result in a more uncertain STW estimate compared to the more traditional approach that has been presented.

$$T(1-t) = R_T \tag{21}$$

A second way to include the thrust measurements is to use thrust identity and find the advance number based on the $K_T(J)$-curve. The rest of the procedure is identical to the STW model based on torque identity, as already described. Because the relative uncertainty in measured thrust is assumed to be four times the relative uncertainty in torque, it is however not recommended to solely depend on the thrust measurement. Thrust sensors are also experienced to be more unstable than torque sensors. The thrust measurement might however reduce the overall uncertainty in the STW estimation if it is rather working as a supplement to the torque measurement. The can be achieved by forming two separate calculations of the advance number J by using both torque- and thrust identity, and establish the final advance number from the average of the two advance numbers. The same case vessel and operational condition has been used to study the effect of including the thrust measurement. In terms of numbers, this means $Q = 150$ [kN m], $n = 108$ [rpm] and $T = 204$ [kN]. The additional input uncertainties to the STW model are listed in Table 12.

The case vessel is still Monte Carlo simulated ($N = 10\ 000$) using the extended STW model. Including thrust measurements in the STW model affects the global sensitivity indices. The updated indices, including the additional input variables from Table 12, are shown in Fig. 6 for both the CP and the FP propeller. For the CP propeller the uncertainty in K_Q, caused by uncertainty in propeller pitch (K_{Q_α}), still has a definite contribution to the overall uncertainty attributing approximately 40% of the global sensitivity. The sensitivity to uncertainty in K_T caused by uncertainty in propeller pitch (K_{T_α}) has a much lower contribution

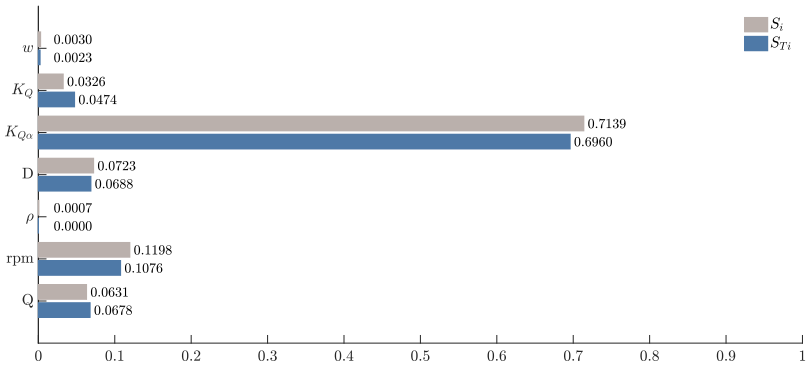

Fig. 4. Global sensitivity indices S_i and S_{Ti} for controllable pitch propeller ($U_\alpha = 1\%$).

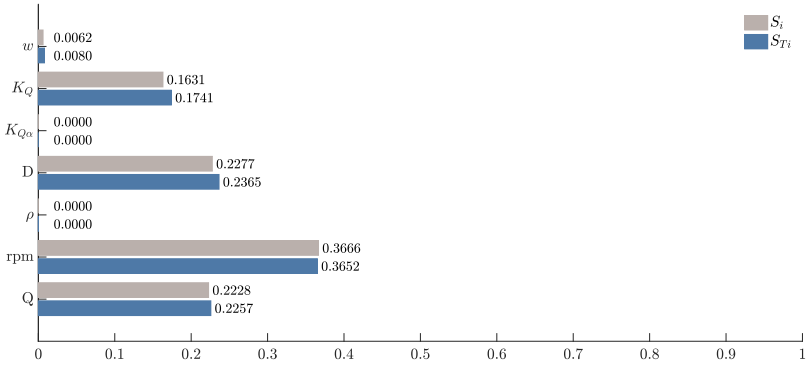

Fig. 5. Global sensitivity indices S_i and S_{Ti} for fixed pitch propeller ($U_\alpha = 0$).

amounting to approximately 10%. This is similar to the contribution from the uncertainty in the thrust sensor. For the FP propeller, the global sensitivity index of the thrust measurement is however significantly higher, amounting to approximately 24%. This makes the thrust measurements the second largest contributor to the global uncertainty in estimated STW.

The Monte Carlo simulation is also used to establish the new expected uncertainty in the estimated STW based on the extended STW model. The results are given in Table 13. The expected STW is still estimated to 12.3 knots, but the standard deviation of estimated STW is reduced to approximately 0.3 knots for the CP propeller as a result of including thrust measurements. This corresponds to 2.4% of the estimated STW. By using a FP propeller, the total uncertainty is 0.21 knots, or 1.67% of the estimated STW, which corresponds to 30.6% reduction in total uncertainty compared to the CP propeller. The reduction in STW uncertainty obtained by including thrust measurements into the STW model is significantly larger when the propeller has a controllable pitch. In numbers, the uncertainty is reduced from 3.65% to 2.40% for the CP propeller, while from 1.96% to 1.67% for the FP propeller. This coincides with the uncertainty factors concerning propeller pitch (K_{Q_α} and K_{T_α}), for which the uncertainty in K_Q is almost 16% higher than the uncertainty in K_T, when evaluated relative to the nominal K_Q and K_T values (K_T is about 5.7 times higher than K_Q at the selected operating point of the case vessel). Including thrust measurements into the STW model is therefore considered to be more attractive for CP propeller installations, simply because potential bias in the full scale propeller pitch angle corresponding to model scale 100% pitch has less contribution to uncertainty in STW when it is affecting K_T compared to K_Q. Careful monitoring of the thrust sensor is however recommended, considering potential issues with such types of sensors that is experienced on full scale installations.

3.4.2. Including waves

Waves will begin to excite ship motions when the size of the waves, relative to the ship, increases. Faltinsen et al. (1980) explained how vessel pitching induces velocities that will increase the effective inflow speed to the propeller. This effect can be expressed as a change in wake fraction, as in Eq. (6). The STW model has been extended to include the effect of waves on the wake fraction. Based on a measured pitching motion (η_5), the amplitude of the motion ($|\eta_5|$) is estimated following Eq. (9) and the encounter frequency (ω_e) is estimated from the frequency of the pitch motion.

Table 13
Resulting parameters of the STW model output for the case vessel, including thrust measurements.

	μ_V [knots]	σ_V [knots]	K_V	S_{KP}
CPP	12.3030	0.2956	−0.04	−0.03
FPP	12.3052	0.2052	−0.05	−0.03

The case vessel is Monte Carlo simulated ($N = 10\ 000$) using the STW model including waves. The pitch motion is pure sinusoidal including noise according to the MRU uncertainty parameters given in Table 8. The amplitude of the sinusoid is set to 5°. The longitudinal distance from the COB to the propeller (L_{PC}) is sampled from the distribution given in the same table. The new sensitivity indices, including η_5 and L_{PC}, are shown in Fig. 7 for both the CP and the FP propeller. The contribution from the uncertainty in the wave related input variables to the total uncertainty is however found to be negligible, with small numbers that may just as well be caused by numerical errors as being actual contributions to the uncertainty in STW. Initially, it may seem odd that the waves have such a small effect on the global uncertainty. However, considering the small effect the wake fraction has on the global uncertainty, the limited contribution from waves on STW uncertainty becomes more reasonable. In short, when the pitch motion amplitude is 5°, the mean increase in water inflow speed to the propeller is small relative to the calm water wake fraction, which means that the additional uncertainty caused by the wave related input variables is cut down. The wake correction in waves will affect the

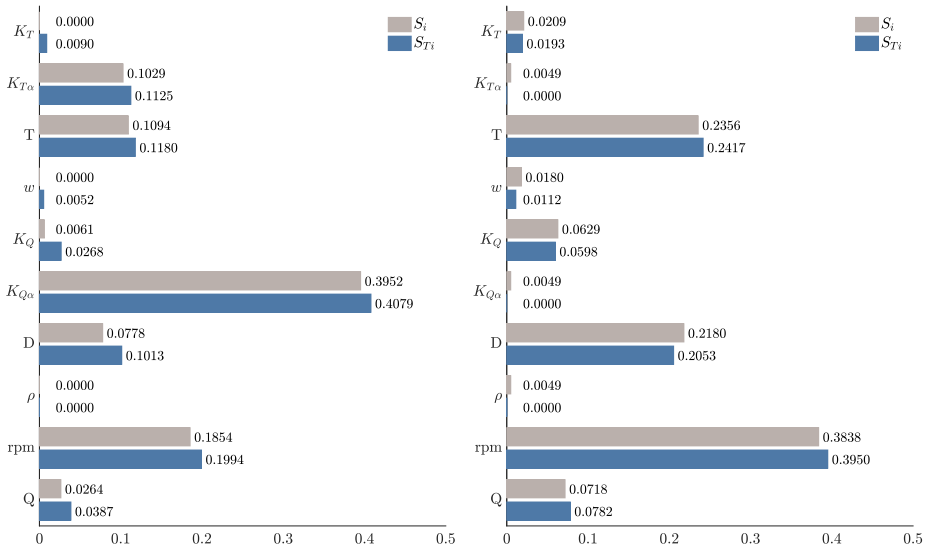

(a) Controllable pitch propeller ($U_\alpha = 1\%$). (b) Fixed pitch propeller ($U_\alpha = 0$).

Fig. 6. Global sensitivity S_i and S_{Ti} of controllable pitch propeller and fixed pitch propeller when adding thrust measurements to the STW model.

estimated STW, but it will not contribute to additional uncertainty in the estimated STW. Because the wave related input variables have limited influence on the uncertainty in STW, the resulting uncertainty parameters of the STW model output including waves are not given.

3.4.3. Uncertainty in scaling of model scale wake fraction

The STW model is based on assuming no uncertainty in the scaling of the wake fraction. This should not be construed as an assertion that the scaling procedure is not uncertain. It is, certainly, uncertain. However, it is found to be very hard to construct an associated uncertainty from which the input to STW model can be sampled from. This means that instead of including some uncertainty that is rather questionable, the resulting uncertainty in the STW model should be evaluated knowing that uncertainty in the wake scaling procedure is omitted.

With that in mind, there are ways to ensure that the uncertainty in the wake scaling procedure in fact can be neglected. By using principles of speed trials, the full scale wake fraction can be calibrated from in-service measurements (Dubois and Binns, 2018), such that the uncertainty in the full scale wake fraction vanishes. During speed trials, double runs are performed in order to account for current, such that SOG, in theory, can be considered equal to the STW. By estimating the water speed through the propeller, following the principle of the STW model, the relative difference in SOG and the estimated speed can be assigned an inaccurate full scale wake fraction. The estimated error between the calculated full scale wake fraction and the scaled model wake fraction can then be used as a calibration factor for the error in the scaling procedure. If the speed trials are performed at a single speed only, the error in wake scaling have to be assumed independent of the forward speed. Note however, that during the speed trial procedure, the calibration factor is in fact considering every possible inaccuracy introduced during the propeller inflow speed estimation, such as the propeller geometry, torque sensor calibration issues etc. It is therefore recommended to ensure that the sensors are properly calibrated prior to this full scale wake calibration. Stating that uncertainty in wake scaling goes to zero is probably too optimistic. However, performing a full scale wake calibration means that the uncertainty introduced through the wake scaling is reduced.

4. Conclusions

Through Monte Carlo simulations of the case vessel using a simple speed through water (STW) model, it is found that the estimated STW has somewhat higher uncertainty than the uncertainty specified by suppliers of traditional Doppler speed logs. Experience in full scale data analysis, combined with concerns in the literature related to the accuracy of speed logs, nevertheless gives the impression that the STW model may provide similar uncertainty as the speed logs. Controllable pitch (CP) propellers are however found to be challenging in terms of the accuracy of the estimated STW, as the uncertainty in full scale propeller pitch is found to have a significant contribution to the total uncertainty in STW. The uncertainty in propeller pitch is not related to manufacturing, but rather the process of configuring the geometrical pitch angle corresponding to 100% pitch in the model tests. The extended STW model including thrust measurements has shown that the STW estimation will benefit from including thrust measurements, particularly for CP propellers, for which it has been found that thrust measurements may decrease the uncertainty in estimated STW by 34.3%. Ships are however rarely equipped with thrust sensors, so the general recommendation is therefore to use the STW model for ships with fixed pitch (FP) propellers.

Based on the simulations, literature and experience, it is expected that the STW model can provide STW data with similar accuracy as Doppler speed logs. Therefore, by using the STW model in combination with a speed log, e.g. by averaging between the two measurements, the uncertainty in the estimated STW can be reduced. Further improvement of the estimated STW from propeller data will require that input variables having large contribution to the total uncertainty in estimated STW, can be measured more precisely. For CP propellers, this basically means ensuring that the full scale 100% pitch is identical to the pitch angle that has been tested in model scale or by numerical simulations. For FP propellers, this means that the sensors measuring rpm and torque should be improved.

In the presence of waves, Doppler speed logs can be erratic and unstable. Small misplacements of the Doppler beam relative to its best position may cause erratic behavior of the speed measurements, either caused by the waves itself or as a result of ship motions that generate air bubbles or acoustic interference with the pulses from the speed log. For some ships it is inevitable to get erratic speed measurements in waves. The uncertainty of the STW model on the other hand, including the change in wake fraction when the ship moves in pitch, was found not to be very much affected by the pitch motion. It is therefore reasonable to rely more on the estimated STW from propeller data when waves are exciting ship motions compared to speed logs, particularly if the speed log already has been providing unstable measurements in waves.

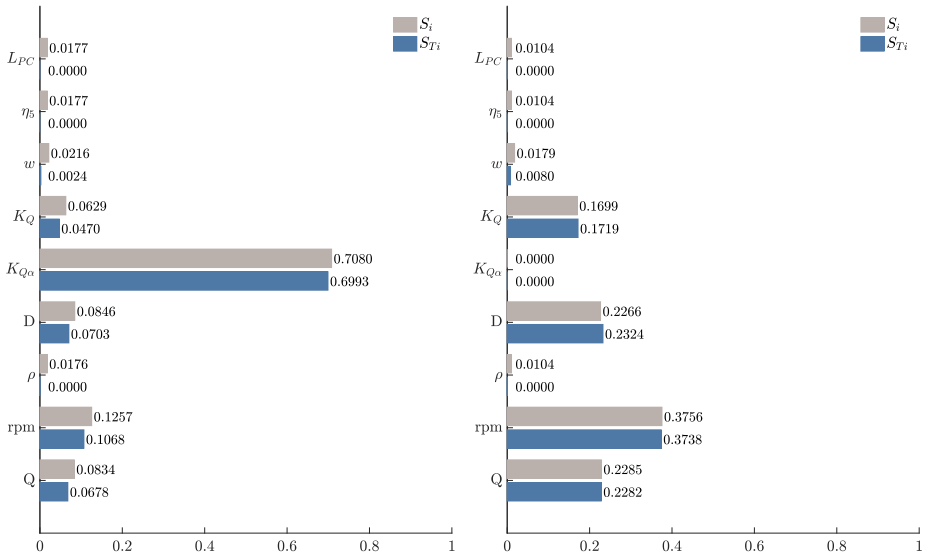

(a) Controllable pitch propeller ($U_\alpha = 1\%$). (b) Fixed pitch propeller ($U_\alpha = 0$).

Fig. 7. Global sensitivity S_i and S_{Ti} of controllable pitch propeller and fixed pitch propeller when including waves in the STW model.

While the proposed method to estimate STW from propeller data is not sensitive to the effect of hull fouling, it is suspect to influence of propeller fouling. A correction for the effect of propeller fouling should be introduced in the future. Since propeller fouling typically develops slowly, a long-term trend in the propeller data might be used to correct for this effect. However, further work is required here.

CRediT authorship contribution statement

Øyvind Øksnes Dalheim: Conceptualization, Methodology, Software, Validation, Formal analysis, Investigation, Data curation, Writing - original draft, Writing - review & editing, Visualization. **Sverre Steen:** Conceptualization, Methodology, Supervision, Funding acquisition, Project administration.

Declaration of competing interest

One or more of the authors of this paper have disclosed potential or pertinent conflicts of interest, which may include receipt of payment, either direct or indirect, institutional support, or association with an entity in the biomedical field which may be perceived to have potential conflict of interest with this work. For full disclosure statements refer to https://doi.org/10.1016/j.oceaneng.2021.109423. Øyvind Øksnes Dalheim reports financial support was provided by Research Council of Norway.

Acknowledgments

The research presented in this paper was carried out in the Kongsberg University Technology Centre "Ship Performance and Cyber-Physical Systems" at the Norwegian University of Science and Technology in Trondheim. It was financed by the project InnoCurrent, which is financed by the Research Council of Norway [grant number 282385] and Kongsberg Maritime.

References

Albretsen, J., Sperrevik, A.K., Staalstrøm, A., Sandvik, A.D., Vikebø, F., Asplin, L., 2011. NorKyst-800. User Manual and technical descriptions.

Antola, M., Solonen, A., Pyörre, J., 2017. Notorious speed through water. In: 2nd Hull Performance & Insight Conference (HullPIC'17). Ulrichshusen, pp. 156–165, URL: http://data.hullpic.info/hullpic2017_ulrichshusen.pdf.

Berman, I., Zereik, E., Kapitonov, A., Bonsignorio, F., Khassanov, A., Oripova, A., Lonshakov, S., Bulatov, V., 2020. Trustable environmental monitoring by means of sensors networks on swarming autonomous marine vessels and distributed ledger technology. Front. Robot. AI 7, 70. http://dx.doi.org/10.3389/frobt.2020.00070, URL: https://www.frontiersin.org/article/10.3389/frobt.2020.00070/full.

Bernitsas, M., Ray, D., Kinley, P., 1981. KT, KQ and Efficiency Curves for the Wageningen B-Series Propellers. Technical Report, Department of Naval Architecture and Marine Engineering. The University of Michigan..

van den Boom, H., Hasselaar, T.W.F., 2014. Ship Speed-Power Performance Assessment. In: SNAME Maritime Convention, Houston.

van den Boom, H., Huisman, H., Mennen, F., 2013. New guidelines for speed/power trials. Level playing field established for IMO EEDI. SWZ Marit. 134, 1–11.

Bos, M., 2016. How metocean data can improve accuracy and reliability of vessel performance estimates. In: 1st Hull Performance & Insight Conference (HullPIC'16). Pavone Canavese, pp. 106–114, URL: http://data.hullpic.info/HullPIC2016.pdf.

Brandsæter, A., Vanem, E., 2018. Ship speed prediction based on full scale sensor measurements of shaft thrust and environmental conditions. Ocean Eng. 162, 316–330. http://dx.doi.org/10.1016/j.oceaneng.2018.05.029, URL: https://www.sciencedirect.com/science/article/pii/S0029801818308047.

Dalheim, Ø.Ø., Steen, S., 2020. Added resistance and speed loss of a ship found using onboard monitoring data. J. Ship Res. 64 (2), 99–117. http://dx.doi.org/10.5957/jsr.2020.64.2.99, URL: http://dx.doi.org/10.5957/jsr.2020.64.2.99.

Dubois, A., Binns, J.R., 2018. Estimation of a ship's nominal wake fraction through full-scale speed trials. In: Proceedings of the 21st Australasian Fluid Mechanics Conference, AFMC 2018, Adelaide.

Faltinsen, O.M., Minsaas, K.J., Liapis, N., Skjørdal, S.O., 1980. Prediction of resistance and propulsion of a ship in a seaway. In: Proceedings of 13th Symposium on Naval Hydrodynamics, Tokyo, pp. 505–529.

Griffiths, G., Bradley, S.E., 1998. A correlation speed log for deep waters. Sea Technol. 39 (3), 29–35.

Guo, B.J., Steen, S., Deng, G.B., 2012. Seakeeping prediction of KVLCC2 in head waves with RANS. Appl. Ocean Res. 35, 56–67. http://dx.doi.org/10.1016/j.apor.2011.12.003.

Hasselaar, T.W.F., den Hollander, J., 2017. Uncertainty of ship speed determination when sailing in waves. In: 2nd Hull Performance & Insight Conference (HullPIC'17). Ulrichshusen, pp. 124–131, URL: http://data.hullpic.info/hullpic2017_ulrichshusen.pdf.

Homma, T., Saltelli, A., 1996. Importance measures in global sensitivity analysis of nonlinear models. Reliab. Eng. Syst. Saf. 52 (1), 1–17. http://dx.doi.org/10.1016/0951-8320(96)00002-6.

IAPWS, 2008. Release on the IAPWS Formulation 2008 for the Thermodynamic Properties of Seawater. Technical Report, Berlin, URL: http://www.iapws.org.

Ikonomakis, A., Galeazzi, R., Dietz, J., Holst, K.K., Nielsen, U.D., 2019. Application of sensor fusion to drive vessel performance. In: 4th Hull Performance & Insight Conference (HullPIC'19). APA, Gubbio, pp. 229–241, URL: http://data.hullpic.info/HullPIC2019_gubbio.pdf.

IMO, 2009. Guidelines for Voluntary Use of the Ship Energy Efficiency Operational Indicator (EEOI). Technical Report, International Maritime Organisation (IMO), London.

IMO, 2011. Amendments to the Annex of the Protocol of 1997 to Amend the International Convention for the Prevention of Pollution From Ships, 1973, as Modified by the Protocol of 1978 Relating Thereto. Technical Report, International Maritime Organisation (IMO), London.

IMO, 2012. Interim Guidelines for the Calculation of the Coefficient f_w for Decrease in Ship Speed in a Representative Sea Condition for Trial Use. Technical Report, International Maritime Organisation (IMO), London.

IOC, SCOR, IAPSO, 2010. The International Thermodynamic Equation of Seawater–2010: Calculation and Use of Thermodynamic Properties. Technical Report 56, Intergovernmental Oceanographic Commission, Manuals and Guides 56, pp. 1–196.

ISO, 1981. ISO R484: Shipbuilding - Ship screw propellers - Manufacturing tolerances - Part 1: Propellers of diameter greater than 2,50 m. Technical Report, (International Organization for Standardization), URL: https://www.iso.org/standard/4527.html.

ITTC, 2002. Propulsion, Propulsor Uncertainty Analysis, Example for Open Water Test. Technical Report, (International Towing Tank Conference, Procedure 7.5-02 03-02.2).

ITTC, 2011. Fresh Water and Seawater Properties. (International Towing Tank Conference, Procedure 7.5-02 01-03), pp. 1–45.

ITTC, 2014a. The Seakeeping Committee. Technical Report, (International Towing Tank Conference), Copenhagen.

ITTC, 2014b. Uncertainty Analysis, Example for Open Water Test. Technical Report, (International Towing Tank Conference, Procedure 7.5–02 03–02.2).

ITTC, 2017a. 1978 ITTC Performance Prediction Method. Technical Report, (International Towing Tank Conference, Procedure 7.5–02 03–01.4).

ITTC, 2017b. Uncertainty Analysis, Example for Propulsion Test. Technical Report, (International Towing Tank Conference, Procedure 7.5-02 03-01.2).

Jansen, M.J.W., Rossing, W.A.H., Daamen, R.A., 1994. Monte Carlo Estimation of uncertainty contributions from several independent multivariate sources. In: Predictability and Nonlinear Modelling in Natural Sciences and Economics. Springer Netherlands, pp. 334–343. http://dx.doi.org/10.1007/978-94-011-0962-8_28, URL: https://link.springer.com/chapter/10.1007/978-94-011-0962-8_28.

Nakamura, S., Naito, S., 1975. Propulsive performance of a container ship in waves. J. Soc. Nav. Archit. Jpn. 15.

Nielsen, U.D., Dietz, J., 2020. Ocean wave spectrum estimation using measured vessel motions from an in-service container ship. Mar. Struct. 69, 102682. http://dx.doi.org/10.1016/j.marstruc.2019.102682.

NORIS Automation GmbH, 2015. Robust temperature sensors for your application. Technical Report, pp. 1–28, URL: https://pdf.nauticexpo.com/pdf/noris-group-gmbh/robust-temperature-sensors-your-application/36035-104509.html{#}open.

Pecoraro, A., Di Felice, F., Felli, M., Salvatore, F., Viviani, M., 2015. An improved wake description by higher order velocity statistical moments for single screw vessel. Ocean Eng. 108, 181–190. http://dx.doi.org/10.1016/j.oceaneng.2015.07.038.

Prytz, G., Gangeskar, R., Bertelsen, V.S., 2019. Distributing real-time measurements of speed through water from ship to shore. In: 4th Hull Performance & Insight Conference (HullPIC'19). Gubbio, pp. 114–127, URL: http://data.hullpic.info/HullPIC2019_gubbio.pdf.

Sadat-Hosseini, H., Wu, P.C., Carrica, P.M., Kim, H., Toda, Y., Stern, F., 2013. CFD Verification and validation of added resistance and motions of KVLCC2 with fixed and free surge in short and long head waves. Ocean Eng. 59, 240–273. http://dx.doi.org/10.1016/j.oceaneng.2012.12.016.

Saltelli, A., Annoni, P., Azzini, I., Campolongo, F., Ratto, M., Tarantola, S., 2010. Variance based sensitivity analysis of model output. Design and estimator for the total sensitivity index. Comput. Phys. Comm. 181 (2), 259–270. http://dx.doi.org/10.1016/j.cpc.2009.09.018.

Saltelli, A., Ratto, M., Andres, T., Campolongo, F., Cariboni, J., Gatelli, D., Saisana, M., Tarantola, S., 2007. Introduction to sensitivity analysis. In: Global Sensitivity Analysis. the Primer, first ed. In: Wiley Online Books, John Wiley & Sons, Ltd, pp. 1–51. http://dx.doi.org/10.1002/9780470725184.ch1, (chapter 1).

Sobol, I.M., 1993. Sensitivity analysis for non-linear mathematical models. Math. Model. Comput. Exp. 1, 407–414.

Taskar, B., Yum, K.K., Steen, S., Pedersen, E., 2016. The effect of waves on engine-propeller dynamics and propulsion performance of ships. Ocean Eng. 122, 262–277. http://dx.doi.org/10.1016/j.oceaneng.2016.06.034.

Taudien, J.Y., Bilen, S.G., 2018. Quantifying long-term accuracy of sonar doppler velocity logs. IEEE J. Ocean. Eng. 43 (3), 764–776. http://dx.doi.org/10.1109/JOE.2017.2735558.

Telfer, E.V., 1927. the Practical Analysis of Merchant Ship Trials and Service Performance. North East Coast Institution of Engineers and Shipbuilders.

Ueno, M., Tsukada, Y., Tanizawa, K., 2013. Estimation and prediction of effective inflow velocity to propeller in waves. J. Mar. Sci. Technol. (Jpn.) 18 (3), 339–348. http://dx.doi.org/10.1007/s00773-013-0211-8, URL: http://www.nmri.go.jp/.

Wanis, P., Brumley, B., Gast, J., Symonds, D., 2010. Sources of measurement variance in broadband acoustic doppler current profilers. In: MTS/IEEE OCEANS. Seattle, http://dx.doi.org/10.1109/OCEANS.2010.5664327.